ELSEVIER

PALAEO

Palaeogeography, Palaeoclimatology, Palaeoecology 165 (2001) 281–297

www.elsevier.nl/locate/palaeo

Sea-level at the Last Glacial Maximum: evidence from northwestern Australia to constrain ice volumes for oxygen isotope stage 2

Yusuke Yokoyama [a,*], Patrick De Deckker [b], Kurt Lambeck [a], Paul Johnston [a], L.K. Fifield [c]

[a] *Research School of Earth Sciences, The Australian National University, Canberra ACT 0200, Australia*
[b] *Department of Geology, The Australian National University, Canberra ACT 0200, Australia*
[c] *Department of Nuclear Physics, Research School of Physical Sciences and Engineering, The Australian National University, Canberra ACT 0200, Australia*

Received 7 December 1999; accepted for publication 17 July 2000

Abstract

New sea-level information from the Bonaparte Gulf in northwestern Australia is used to constrain the magnitude and rates of change of ice volumes during the Last Glacial Maximum (LGM). The region is tectonically stable and far from the former ice-covered regions. The glacio-hydro-isostatic adjustment of the coast is therefore relatively small, and the corrections for this effect are not sensitive to details of the rebound model. Microfossil analysis and AMS radiocarbon dating of 11 gravity cores taken across the shelf and Bonaparte Gulf demonstrate that: (1) the LGM sea-levels were locally at -125 ± 4 m; (2) the LGM terminated abruptly at 19 000 cal yr BP with a rapid rise in sea-level of about 15 m over the next 500 years; and (3) the onset of the minimum sea-levels occurred before 22 000 cal yr BP. When corrected for the glacio-hydro-isostatic effects, the increase of LGM ice volumes over the present-day ice volume is 52.5×10^6 km^3. The termination of the LGM is marked by a rapid ice discharge of 5.2×10^6 km^3.

Keywords: AMS; Bonaparte Gulf; Foraminifera; ice volume; Last Glacial Maximum; Ostracoda; radiocarbon dating; sea-levels

1. Introduction

The volume and geographic distribution of the ice during the Last Glacial Maximum (LGM) and the subsequent Late-glacial period remain uncertain quantities despite recent progress in understanding the evolution of the large Late Pleistocene ice sheets. Some constraint on the total volumes of ice locked up in these ice sheets is provided by observations of past sea-levels (see Table 1), but such data have remained uncertain because of the limitations of the observational record and because of the necessity to correct such data for both isostatic and tectonic displacements of the crust.

Nakada and Lambeck (1988) reviewed the

* Corresponding author. Present address: Space Sciences Laboratory, University of California Berkeley and Geosciences and Environmental Technology Division, Lawrence Livermore National Laboratory, 7000 East Avenue, PO Box 808, L-202, Livermore, CA 94550, USA. Tel.: +1-925-424-5450; fax: +1-925-422-1002.
E-mail address: yusuke@ssl.berkeley.edu (Y. Yokoyama)

0031-0182/01/$ - see front matter
PII: S0031-0182(00)00164-4

Table 1
Some published sea-level values for the LGM

Reference	Sea-level[a] (m)	Locality or method[b]
Nakada and Lambeck (1988)	130[a]	Isostatically corrected data from intermediate- and far-field
Tushingham and Peltier (1991)	115[c]	Isostatically corrected data mainly from near- and intermediate-field
Peltier (1994)	105[c]	Data from Barbados corrected for isostasy but not for tectonics
Fleming et al. (1998)	125[a]	Isostatically and tectonically corrected data from intermediate- and far-field
Hughes et al. (1981)	127–163[a]	GL
Chappell and Shackleton (1986)	130[a]	$\delta^{18}O$
van Andel and Veevers (1967)	120–130	Timor Sea, sed
Jongsma (1970)	150–175	Arafura Sea, sub.Ccoral
Veeh and Chappell (1970)	120	PNG, up.Coral
Carter and Johnson (1986)	114–133	GBR, sed
Fairbanks (1989), Bard et al. (1990)	117	Barbados, dr.Coral
Ferland et al. (1995)	<130	off Sydney, sed
Colonna et al. (1996)	145	Mayotte, sub. Coral

[a] Ice volume equivalent sea-level.
[b] GL: Glaciological method; $\delta^{18}O$: Foraminiferal $\delta^{18}O$ record obtained from deep-sea sediment core. GBR: the Great Barrier Reef; PNG: Huon Peninsula, Papua New Guinea sed: sediment core taken from sea floor; up.Coral: uplifted coral reefs; dr.Coral: drilled coral obtained from offshore; sub.Coral: coral obtained by submergible from sea floor.
[c] This refers to eustatic sea-level. The ice-volume-equivalent sea-level would be about 20% greater.

limited available data and concluded that, globally, sea-level at the LGM was some 130 m lower than present. Table 1 summarizes some observational estimates of sea-levels at sites far from the former ice sheets at the time of the LGM. New data from Barbados, however, led to the conclusion that this level may have been about 120 m below the present level (Fairbanks, 1989; Bard et al., 1990), whilst others have argued that from the same observational evidence, this may have been only about 105 m (Peltier 1994). These differing estimates of the Last Glacial Maximum sea-level have major glaciological implications and improved estimates are clearly desirable.

The Australian margin is well suited for studies of sea-level change during the LGM. The margins are tectonically stable, as witnessed by the occurrence of Last Interglacial Shorelines (OIS; Marine Oxygen Isotope Stage -5e) near the present-day sea-level (Marshall and Thom, 1976; Stirling, et al., 1995, 1998). Also, the continent lies far from the former ice sheets such that the isostatic corrections, due mainly to the hydro-isostatic effects, are small and not strongly dependent on the details of the ice-load geometry. Finally, there are wide and shallow shelf areas with depressions where conditions may have been favourable for the preservation of evidence for former and now submerged shoreline positions. The Timor Sea, and Northwest Shelf as well as the Arafura Sea (Fig. 1) provide environments suitable for sea-level studies and this area has provided one of the few reliable estimates of sea-level at the time of the LGM (van Andel and Veevers, 1967; van Andel et al., 1967).

In this paper, we report on new data that provide evidence for sea-levels during the OIS 2 as well as for the period leading to the LGM. The data are based on core and dredge samples from numerous localities in the Timor Sea (Fig. 1) that probably existed as lagoonal or very shallow coastal environments when sea-levels were much lower. Shallow marine molluscs and brackish lagoonal microfossil remains have been identified and radiocarbon-dated to determine the relative sea-levels about the time of the LGM.

These observations have then been combined with the results of glacio-hydro-isostatic modelling to estimate ice equivalent sea-level (isl) change and the volumes of land-based ice which were present over and above the present-day volumes.

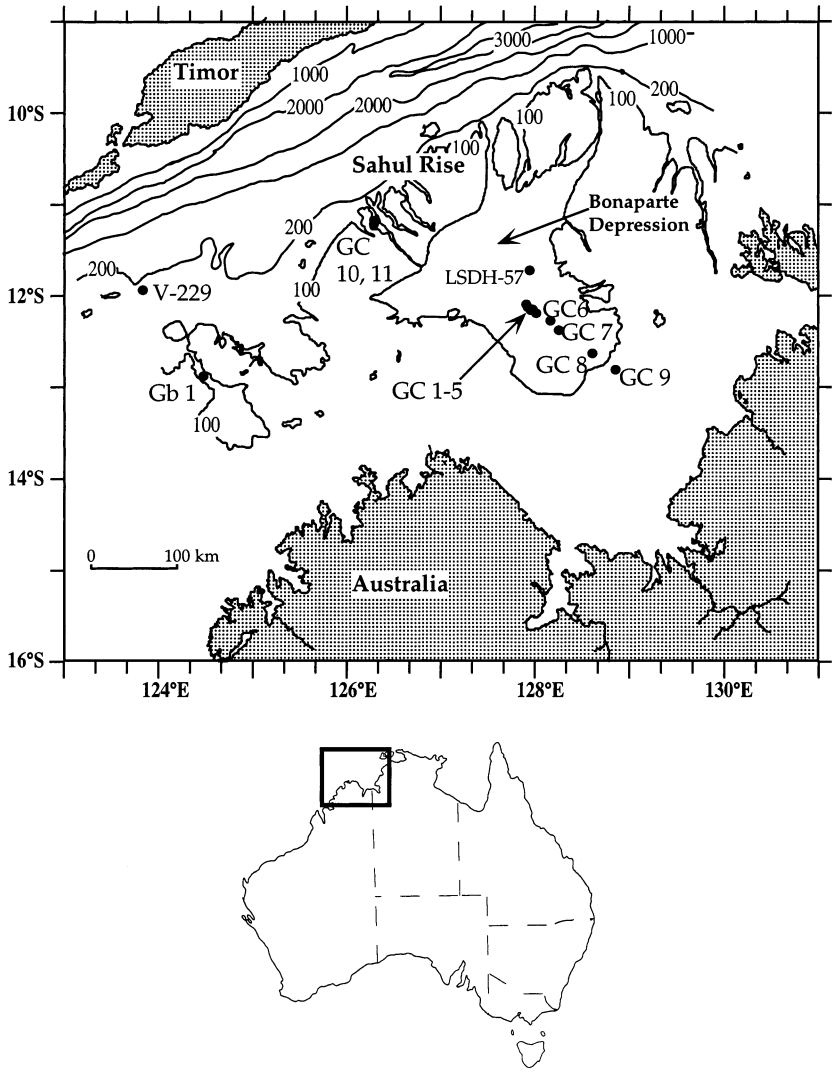

Fig. 1. Map showing the location of the Timor Sea with bathymetric contours in metres. Filled circles represent sampling sites for the present study, except for LSDH-57 and V-229 previously reported by van Andel and Veevers (1967).

2. New observational evidence for Last Glacial Maximum sea-levels

2.1. Regional setting

The Timor Sea, located off the northwestern coast of Australia, includes a broad and well-developed shallow continental shelf, the Sahul Shelf, and local bathymetric depressions of which the Bonaparte Gulf is the largest. During times of sea-level lowstand, much of the shelf was exposed, and its outer edge would have provided protection against wave action for sediments which accumulated in shallow water depression. At these times, the deepest part of the Gulf, called the Bonaparte Depression, was connected to the open ocean via narrow channels and, depending on the sea-level, may have oscillated between marine and near-freshwater conditions.

A total of 23 gravity cores, 10 vibro cores and

three dredge sedimentary samples were collected in water depths ranging from 34 to 147 m as part of a wider sedimentological investigation in the area. Among the gravity cores, nine were taken from the Bonaparte Depression. The location of these and other shallow water cores are illustrated in Fig. 1 and Table 2, along with the locations of two cores discussed by van Andel et al. (1967).

2.2. Analytical methods

Lithological descriptions of all retrieved cores were made and 11 gravity cores were selected for detailed micropalaeontological analysis, principally of foraminifera and ostracods. Remains of calcareous organisms were radiocarbon-dated depending on the sample size, by either scintillation counting (LSC) or accelerator mass spectrometry (AMS) methods. The conventional dates were obtained using standard procedures of the Australian National University (ANU) radiocarbon laboratory (Gupta and Polach, 1985). For AMS dates, samples were prepared in a newly built graphitisation line (Yokoyama, 1999; Yokoyama et al., in press) which catalytically condensed graphite with iron in a hydrogen atmosphere (Vogel, et al., 1984). The dates were obtained using the ANU's 14UD accelerator (Fifield et al., 1992). The AMS samples were selected using a standard micropalaeontological microscope and then ultra-sonically cleaned in distilled water. Strong acid etching was undertaken for all samples to eliminate secondary carbon contamination of the sample. Original sample sizes were more than 1.5 times that normally required so the first portion of CO_2 collected, corresponding to about 30–40% of the total sample, could be discarded so as to minimize any possible secondary carbon contamination of the calcium carbonate skeleton. Quality control of the current system has been made by repeated measurement of the IAEA C-1 and the ANU sucrose, which are widely used as international standard material with no ^{14}C and modern reference amount of ^{14}C, respectively. The range of the background ^{14}C level so far is from 0.04 pM (percent modern) to 0.3 pM, which corresponds to 63 400–46 600 ^{14}C yr BP. The AMS facility of ANU has better than a 2% precision (Yokoyama, 1999; Yokoyama et al., in press). Consequently, samples as old as 45 000 ^{14}C yr BP can be measured in the current system. All ^{14}C ages have been calibrated to a calendar time scale (see Table 3 for details). We describe hereafter ^{14}C dates by denoting '^{14}C yr BP'; otherwise, we use the calendar time scale.

Table 2
Location of the cores and grab samples discussed in the present study

Sample[a]	Longitude E	Latitude S	Water depth (m)	Sampling method
GC 1	127° 55.00′	12° 06.00′	127	Gravity core
GC 2	127° 55.03′	12° 06.02′	128	Gravity core
GC 3	127° 56.02′	12° 07.00′	127	Gravity core
GC 4	128° 00.00′	12° 09.99′	121	Gravity core
GC 5	128° 01.50′	12° 11.00′	118	Gravity core
GC 6	128° 09.99′	12° 18.00′	110	Gravity core
GC 7	128° 15.99′	12° 22.96′	107	Gravity core
GC 8	128° 37.04′	12° 38.36′	95	Gravity core
GC 9	128° 52.00′	12° 50.01′	88	Gravity core
GC 10	126° 19.53′	11° 12.46′	103	Gravity core
GC 11	126° 17.49′	11° 13.85′	101	Gravity core
Gb 1	124° 28.89′	12° 54.96′	129	Dredge
V-229[b]	123° 50.40′	11° 57.50′	132	Dredge
LSDH-57[b]	127° 57.00′	11° 44.00′	132	Piston core

[a] GC1-11 are stored at Australian Geological Survey Organisation (AGSO), and Gb1 is at Australian National University.
[b] van Andel and Veevers (1967).

Table 3
^{14}C results

Core	Water depth (m)	Depth in core (cm)	^{14}C age[a]	Calendar age[b]	Sample ID[c]	Dated material[d]
GC 2	128	23	9770 ± 100	11 190 ± 40	ANUA-7518	B, F
		434	39 240 ± 600	44 960 ± 630	ANUA-7514	F
GC 3	127	87	11 810 ± 130	13 790 ± 260	ANUA-7516	B
		130	24 100 ± 230	28 330 ± 260	ANUA-9304	B
		140	25 200 ± 250	29 580 ± 290	ANUA-9305	B
		160	24 750 ± 440	29 070 ± 500	ANUA-9506	B
		186	25 550 ± 300	29 980 ± 340	ANUA-6806	B
		455	30 430 ± 380	35 450 ± 420	ANUA-6929	F
GC 4	121	60	8040 ± 110	8890 ± 170	ANUA-8815	B
		180	16 730 ± 250	19 940 ± 420	ANUA-8816	B
		210	18 390 ± 200	21 690 ± 240	ANUA-9318	B
		240	24 060 ± 240	28 280 ± 280	ANUA-9303	B
		350	30 730 ± 310	35 780 ± 340	ANUA-9302	B
GC 5	118	42	11 410 ± 180	13 470 ± 310	ANUA-6900	F
		113	14 160 ± 200	16 980 ± 330	ANUA-8813	B
		227	16 240 ± 240	19 370 ± 410	ANUA-6928	F
		227	16 540 ± 170	19 720 ± 370	ANUA-6807	B
		229	16 690 ± 190	19 890 ± 380	ANUA-7531	F, B
		320	17 360 ± 230	20 480 ± 270	ANUA-6930	F, B
		340	18 040 ± 150	21 280 ± 180	ANUA-9317	B
		353	25 750 ± 300	30 210 ± 340	ANUA-8812	B
		453	32 630 ± 480	37 870 ± 520	ANUA-8820	B
GC6	110	35	15 070 ± 160	18 030 ± 320	ANUA-9404	B
		40	15 980 ± 170	19 080 ± 350	ANUA-9324	B
GC 7	107	26	14 720 ± 160[L]	17 630 ± 310	ANU-10750	*Cf*
		35	14 910 ± 210[L]	17 850 ± 360	ANU-10747	*Cf*, *Pu*
		44	15 880 ± 160[L]	18 960 ± 350	ANU-10746	*Cf*, *Pu*, *Mj*
GC 8	95	40	4180 ± 70	4710 ± 130	ANUA-9404	B
		110	11 590 ± 180	13 620 ± 210	ANUA-9319	B
		220	28 780 ± 370	33 610 ± 410	ANUA-9403	B
		300	28 560 ± 390	33 370 ± 440	ANUA-9320	B
		327	35 600 ± 800	41 090 ± 860	ANUA-9402	B
		358	32 710 ± 620	37 960 ± 680	ANUA-9405	B
GC 9	88	104	42 920 ± 720	48 800 ± 740	ANUA-9410	B
		115	40 930 ± 760	46 730 ± 790	ANUA-9409	B
		130	48 370 ± 1 180	54 330 ± 1 180	ANUA-9408	B
		160	34 800 ± 530	40 230 ± 570	ANUA-7517	F
GC 10	103	287	14 750 ± 150	17 660 ± 310	ANUA-7520	F
GC 11	101	185	14 570 ± 180	17 450 ± 320	ANUA-7519	F
Gb 1	129	Surface	14 900 ± 150[L]	17 830 ± 310	ANU-10429	MIX
		Surface	18 630 ± 150[L]	21 980 ± 180	ANU-10430	*Ap*
V-229	132	Surface	16 910 ± 500[L]	20 140 ± 660	LJ-516	*Cs*
LSDH-57	132	97–104	17 400 ± 1 000[L]	20 520 ± 1190	LJ-998	Silty clay
		201–208	18 900 ± 1 500[L]	22 290 ± 1,760	LJ-999	Silty clay

[a] All dates are calculated using the half-life of 5568 years expressed in yr before 1950 (BP). The errors are one standard deviation of counting. Superscript 'L' indicates that the result was obtained with conventional liquid scintillation counting method. Others were obtained with AMS.

[b] Ages obtained using Calib 4.1 (Stuiver et al., 1998) and a second-order polynomial approximation (Bard et al., 1998), for the ^{14}C ages younger and older than 17 000 ^{14}C yr BP, respectively. Statistical errors are given at the one sigma level.

[c] Numbers with prefixes 'ANU' and 'ANUA' were dated at the Quaternary Dating Laboratory and Nuclear Physics Department in ANU, respectively. 'LJ' were dated at the La Jolla radiocarbon laboratory (van Andel et al., 1967).

[d] B: bivalves; F: benthic foraminifera; *Cf*: *Ctenocardia fornicarta*; *Pu*: *Paphia undulata*; *Mj*: *Marca japonica*; MIX: mixtures of shells, forams, calcareous algae; *Ap*: *Antigona puerpera*; *Cs*: *Chlamys senatorius*.

2.3. Results

2.3.1. Sample descriptions

The surface sediments in Bonaparte Gulf are of two kinds: carbonate-rich sand and silty clay (Van Andel and Veevers, 1967). Lithological logs of the selected cores are provided in Fig. 2. Core samples from the Bonaparte Depression are dominated by very dark brown to black colours (7.5YR 2/4 to 2.5YR 2/0). With the exception of GC9, which is dominated by silt, all cores consist primarily of clay to silt-sized grains. The two cores from the outer edge of the shelf (GC10 and GC11) consist of coarser, mainly silt-sized sediments grey to olive in colour. The three dredge samples from Gb 1 (see Fig. 1) mostly comprise calcareous sand to gravel-sized grains.

2.3.2. Micropalaeontological indicators of environmental conditions

Although the area has a high production rate for diatoms (e.g. Burford et.al., 1995), few fossil diatoms were found in the gravity cores, probably as a result of post-depositional silica dissolution (e.g. Hurd, 1973; Johnson, 1974; McManus et al., 1995). Siliceous skeletons were also rare in the LSDH-57 core, also from the Bonaparte Depression, examined by van Andel et al. (1967) (see Fig. 1). Benthic foraminifera and ostracods (and pteropods) are common in the cores at some levels.

The environmental interpretations inferred from the faunal assemblages are summarised in Fig. 3. Well-preserved planktonic foraminifera and pteropods, found in the upper parts of the cores (see Fig. 3), are indicative of an open-marine facies, and their occurrence is coincident with marine ostracods such as *Argilloecia* sp. and *Bradleya* sp. No freshwater ostracods were observed in any of the cores, but the euryhaline ostracod taxa *Cyprideis* and *Leptocythere*, indicative of brackish water with possibly some freshwater influence/mixing (De Deckker, 1988; Yassini and Jones, 1995), have been identified. The state of preservation of the valves of these ostracods provides further information on their transport history (see De Deckker, 1988 for more information). The occurrence of the typically estuarine foraminifers *Ammonia beccarii* and *Elphidium* sp. is a further indication of brackish-water conditions (e.g. Albani, 1979; Cann and De Deckker, 1981; Murray, 1991; Hayward and Hollis, 1994; Yassini and Jones, 1995). Bivalve molluscs and gastropods have also been used to establish palaeoenvironmental conditions.

Based on a combination of faunal assemblages, four environmental facies have been identified:

Open marine (oM): definitive presence of the fragile pteropods, numerous benthic ostracod and foraminifer taxa, all being indicative of normal sea-water salinity and water depths greater than about 20 m. Specimens usually well preserved. Planktic foraminifers are rare due to the shallow bathymetry of the Gulf.

Shallow marine (sM): presence of numerous and usually well-preserved benthic foraminifera and marine ostracod taxa, which include *Aglaiella*, *Argilloecia*, *Callistocythere*, *Loxoconcha*, *Pterygocythereis*, *Uroleberis*. In addition, bairdiid ostracods are common. Terrigenous components are rare; presence of bryozoan and echinoid spine remains and holothurian spicules; all these are indicative of normal sea-water salinity and water depths less than $\sim$10 m. Pteropods are absent in these samples.

Marginal marine (mM): low diversity of benthic marine ostracod commonly *Neocytheretta* ssp., *Xestoleberis*, and foraminifer taxa accompanied by scaphopods, all of which show signs of abrasion; bivalves molluscs are abundant and often damaged; frequent occurrence of terrigenous material: these are indicative of water depths well below 5 m, being within the tidal zone influence with salinities fluctuating from normal sea-water values.

Brackish (Br): paucity of typically marine foraminifera and ostracod taxa; presence of Ammonia beccarii often in large numbers and usually in minute (dwarf) sizes as a result of environmental stress (e.g. high temperature, low salinities), *Leptocythere* sp., *Neocytheretta* spp., *Cyprideis australiensis*; common signs of 'bleaching' of the calcareous shells by corrosive waters; terrigenous particles (mostly clays), organic (vegetal) fibres, and insect remains forming a substantial fraction of the sample. All these are indicative of salinities

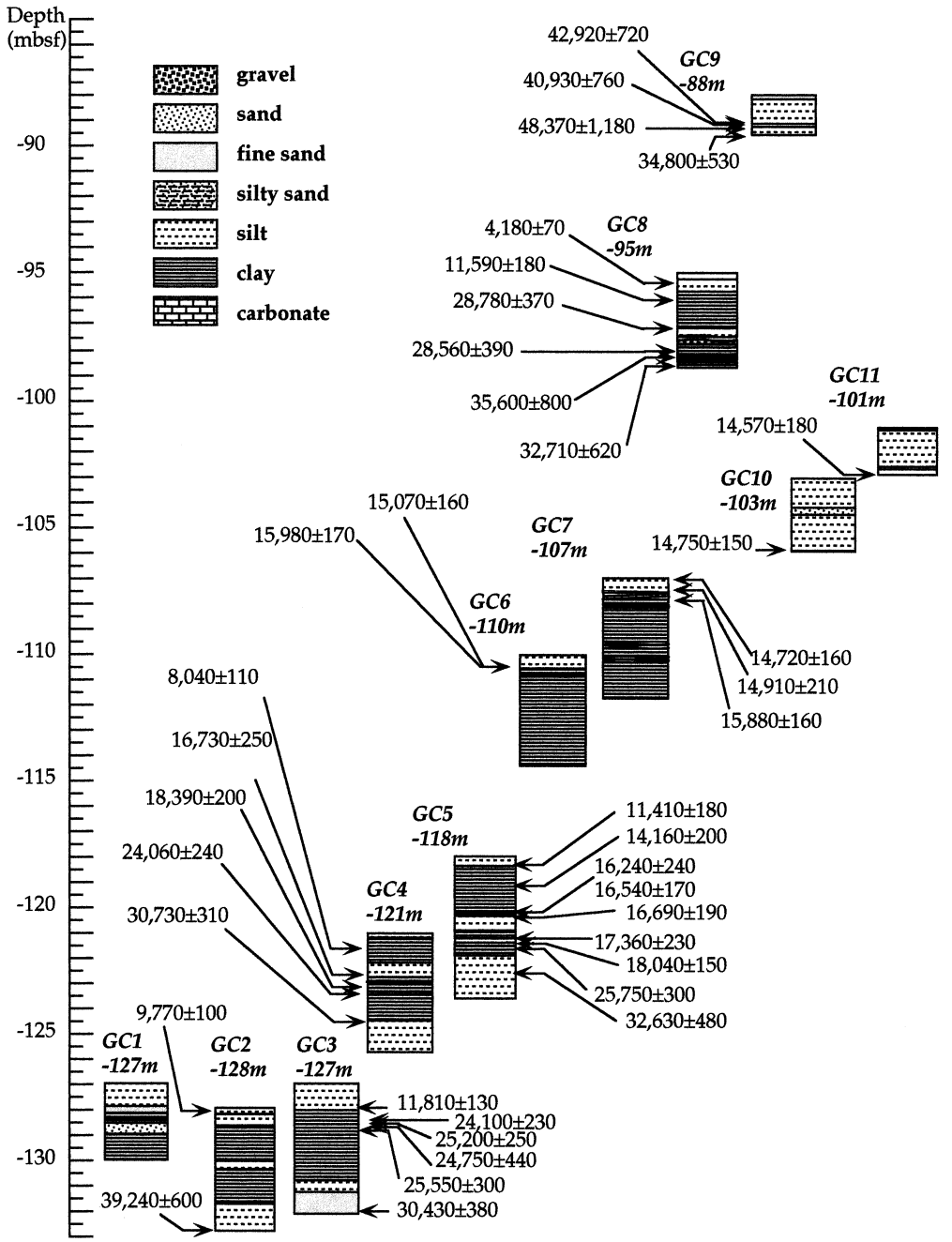

Fig. 2. Columnar sections of gravity cores obtained from the Bonaparte Gulf for the present study. Cores were collected from −88 to −128 m water depth so that they contain preserved sea-level information for the LGM. Note that most of ^{14}C ages are stratigraphically in order, confirming that reworking of sediments has been unlikely. Numbers show radiocarbon dating results in ^{14}C yr BP.

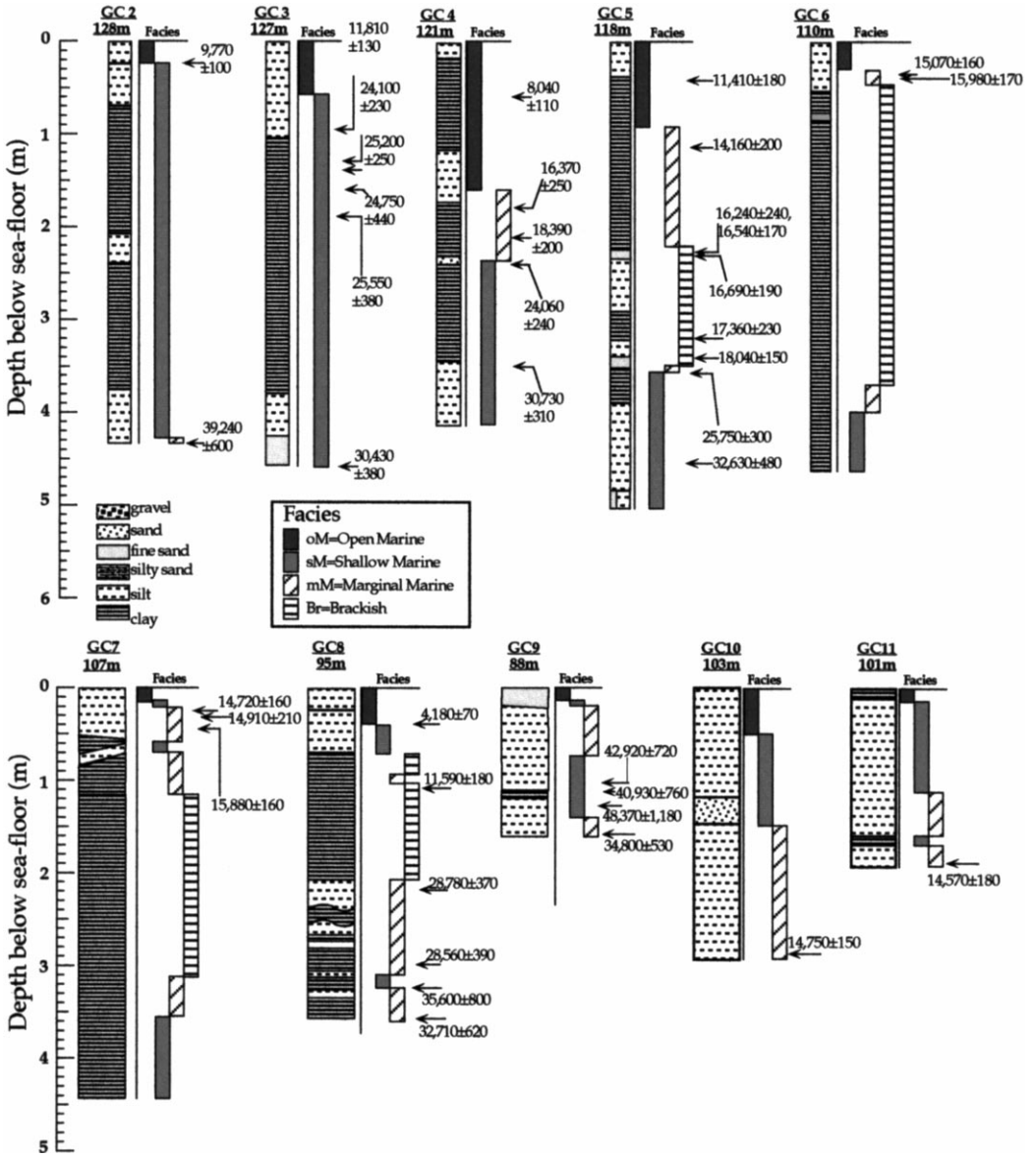

Fig. 3. Sedimentological description of the cores with facies inferred from micropalaeontological characteristics (see Section 2.3.2) and ^{14}C dates for the cores. Numbers show radiocarbon dating results in ^{14}C yr BP.

well below normal sea-water and strongly influenced by continental waters.

The approach that we have taken in this paper to reconstruct the sea-level change, and pinpoint the lowest sea-level at any site, is to examine the different facies in a sequence in a core so as to determine with confidence the shallowest water depth, the latter being of significance for determining the sea-level curve.

2.3.3. Radiocarbon dating results

Table 3 summarizes the radiocarbon dates for selected horizons in nine of the gravity cores, one grab sample and three dates from van Andel

and Veevers (1967) core LSDH-57 and V-229. Reservoir (400 years) and $\delta^{13}C$ corrections have been applied, and calendar ages were obtained using the Calib 4.1 conversion (Stuiver et al., 1998) for ages up to 17 000 ^{14}C yr BP and using a polynomial relationship between the two time scales for older material (Bard et al., 1998).

2.3.4. *Micropalaentological results*

In this section, we discuss the micropalaeontological results of cores in order of decreasing water depth.

The microfaunal composition of core GC3 was examined in detail for 14 horizons. Core GC1 was not analyzed in detail, being very similar to cores GC2 and GC3. The upper-most part of the core is characterised by sediments deposited in an open-marine environment with a change to shallower water conditions occurring at about 60 cm and a further change to a marginal marine environment at about 95 cm. A radiocarbon date for this boundary/change gave 11 810 $\pm$ 130 ^{14}C yr BP. Environmental conditions remained similar back to 25 500 $\pm$ 380 ^{14}C yr BP at which point a return to shallow marine conditions occurred. Nowhere in this interval is there any evidence that brackish-water conditions occurred or that the site was subaerially exposed. Shallow-marine conditions persisted down to the base of the core, which is dated at 30 430 $\pm$ 380 ^{14}C yr BP. Core GC2, being essentially located at the same water depth, provides a similar environmental reconstruction down-core with decreasing water depth from open marine to marginal marine conditions, followed by a return to shallow marine conditions. In both cores, the silty sediments correspond mainly to the open-marine environment within the depression during the Holocene interval, whereas the clay sediments correspond mainly to the last deglaciation and the glacial maximum period.

Core GC4, from a somewhat shallower depth, exhibits a similar sequence with respect to the inferred environmental conditions mentioned above, except that the transition in the upper part of the core goes from open marine directly to marginal marine without a well-developed intervening shallow marine condition. This transition occurs at about 16 000 ^{14}C yr BP. The lower part of GC4 contains shallow marine facies. The level of transition from shallow marine to marginal marine facies is about 240 cm in depth in the core at about 24 060 ^{14}C yr BP. Core GC5 records a brackish-water environment, and this condition persisted from about 16 000 ^{14}C yr BP to at least about 18 000 ^{14}C yr BP. The deepest level of the brackish facies in the core lies above a marginal marine facies overlying the shallow marine facies. The lowest part of the core, below 365 cm, is characterised by the presence of marine ostracods and planktonic foraminifera. Above 340 cm, small *Ammonia beccarii* occur along with other shallow-water to brackish indicators such as *Elphidium* sp. and *Cyprideis australiensis*. Some of the horizons in this section also contain scaphopods and marine molluscs, thus indicating a transition to marginal-marine conditions.

Fig. 4 illustrates the depth-age relationship of the radiocarbon samples from GC5. For the interval between about 40 and 340 cm, corresponding to the beginning of the Late Glacial stage, the sedimentation rate was relatively constant and high (59 cm/^{14}C kyr) and then slowed down above 113 cm depth (26 cm/ ^{14}C kyr). The two dates near 227 cm depth relate to one fraction consisting of foraminifera species only (16 240 $\pm$ 240 ^{14}C yr BP) and the other fraction consisting of small bivalve molluscs (16 540 $\pm$ 170 ^{14}C yr BP), both from the same horizon. The age agreement within the experimental error indicates that both fractions represent true 'depositional ages'. A hiatus occurs

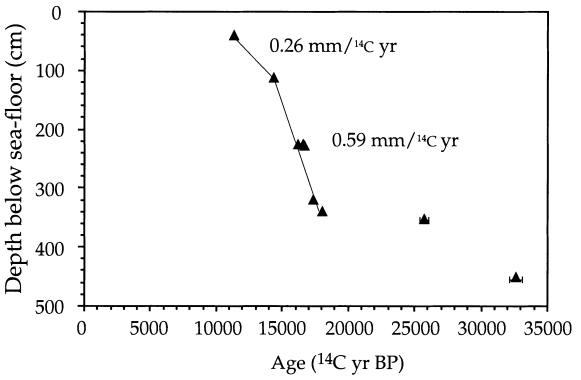

Fig. 4. Depth and ^{14}C dates in the core GC5. Sedimentation rates obtained from slope of lines.

below this horizon, lasting from about 18 040 to 25 750 ^{14}C yr BP, corresponding approximately to the time of the maximum glaciation recorded elsewhere at high latitudes (eg., Clapperton, 1997). This hiatus is interpreted to have been caused by erosion of a sub-aerially exposed surface rather than being due to a starvation of sediment supply, since the nearby cores in somewhat deeper waters do not exhibit such a phenomenon. Similar hiatus are observed from sedimentological analysis in shallower coves. These are also perhaps due to sub-aerial exposure during the low sea-level period (Fig. 3).

Core GC6 also contains brackish and marginal marine microfossil indicators. ^{14}C dates obtained from the horizon at 40 cm depth below the top of the core indicate that marginal marine conditions existed at 15 980 $\pm$ 170 ^{14}C yr BP. This is the lowest occurrence of the marginal marine facies in the upper part of GC6. Facies below this depth indicate brackish environments and coincide with the appearance of clay size sediments. Facies and dating results inferred from GC6 are in very good agreement with GC5.

Core GC7, from a water depth of 107 m, contains a mixture of well-preserved shallow water bivalves, including *Paphia undulata*, *Marcia japonica,* and *Ctenocardia fornicata*, which together indicate a littoral sand habitat (Lamprell and Whitehead, 1992). The three conventional radiocarbon ages are also sequentially in order, thus indicating that the sediments have not been disturbed. The AMS ages of the lowest horizon in cores GC10 and GC11 are similar to these ages. Core GC8 and 9, some 10–20 m shallower than GC7, however, contains age reversals that are suggestive of reworking.

The dredged surface sample Gb1 contains the bivalve mollusc *Antigona puerpera* (Lamprell and Whitehead, 1992) whose characteristic habitat is littoral sand. A specimen with both valves is well preserved, suggesting that it is not reworked. With an age of 18 630 ^{14}C yr BP, this sample implies that the LGM sea-level was above $-$129 m. The second sample dated from Gb1 consists of a mixture of different bivalves living at various water depths, including *Lima lima* and *Antigona puerpera*. Their age of 14 900 $\pm$ 450 ^{14}C yr BP is significantly less than that of the hinged bivalve sample, suggesting that reworking has transported some material from shallower sites.

Sea-levels during the Late-glacial are also recorded in the cores from both the outer edge of the shelf (GC10, 11) and the Bonaparte Depression. For example, analysis of microfossils from GC10 and GC11, at $-$103 m and $-$101 m, respectively, indicates a marginal marine environment such as a beach or coastal lagoon at between 14 750 $\pm$ 170 and 14 570 $\pm$ 180 ^{14}C yr BP. A similar inference is drawn from the upper part of GC7 where, at $-$105 m, littoral-dwelling bivalves, such as *Ctenocardia fornicata*, *Paphia undulata* and *Marcia japonica*, yield a radiocarbon age of 14 600 ^{14}C yr BP. Sea-levels predating the LGM period are recorded in several cores; viz. GC2, GC3, GC5, GC8 and GC9.

2.3.5. Discussion

Core GC5 provides the most direct evidence for the position of sea-level during the time of maximum glaciation, with brackish, shallow-water conditions indicated between 18 040 $\pm$ 150 and about 16 000 ^{14}C yr BP, overlying a hiatus that extended from 25 750 $\pm$ 300 to 18 040 $\pm$ 150 ^{14}C yr BP (Fig. 3). This hiatus is attributed to a time of subaerial exposure of the sediments, indicating that during this time, the local sea-level was below $-$121 m. The brackish-water conditions, such as those identified at about 17 500 ^{14}C yr BP, indicate that at this time, sea-level was only a few meters above $-$121 m. The dredged surface sample Gb 1 indicates sea-level was above $-$129 m at 18 630 ^{14}C yr BP. These results are similar to the results obtained previously by van Andel et al. (1967) from a nearby piston core, LSDH-57 at a water depth of 132 m. Marine silty clays in that core gave radiocarbon ages of 17 400 $\pm$ 1000 and 18 900 $\pm$ 1000 ^{14}C yr BP (van Andel et al., 1967), thus indicating that sea-levels were above this depth for the time interval encompassed by these two dates. The littoral-living bivalve *Chlamys senatorius* dredged from $-$132 m (V-229, Fig. 1) on the outer edge of the Sahul shelf by van Andel et al. (1967) indicates that sea-level was above this position at 16 910 $\pm$ 500 ^{14}C yr BP.

Fig. 5 illustrates the height–age relationship for

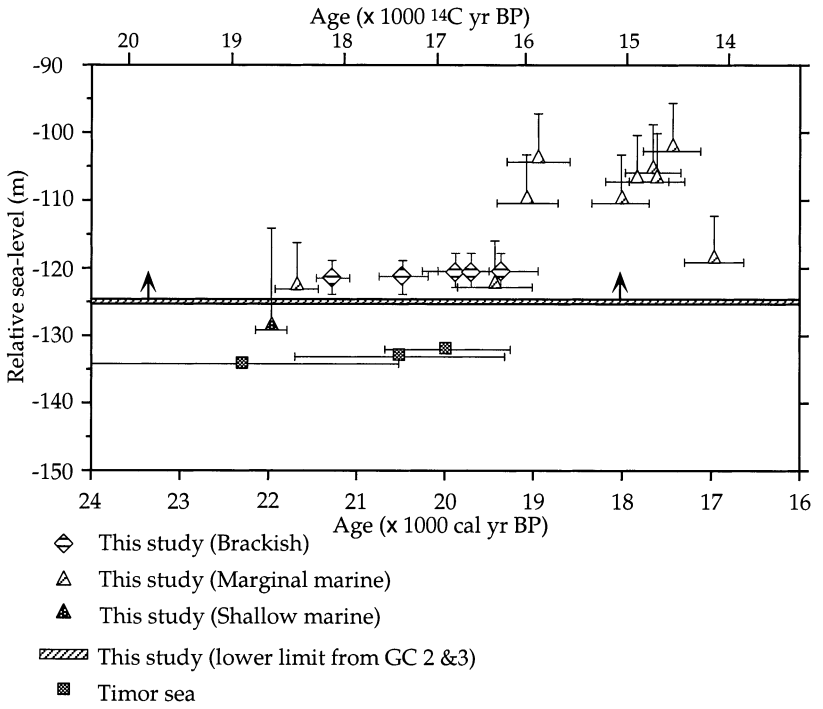

Fig. 5. Relative sea-level data from the present study together with previously reported data from Timor Sea (van Andel and Veevers, 1967). The shaded horizontal bar indicates the lower limit of sea-level inferred from the deepest cores in the region. The sea-level must lie above this limit because shallow-water facies have not been recognised in both cores GC2 and GC3. This implies that the sites of those cores must have never been above water for the period of consideration here.

the data from the Bonaparte Depression. The results indicate that sea-levels were locally below −121 m and above −125 m during the LGM, followed by a rise to above −105 m by about 14 750 ^{14}C yr BP. Sea-levels first fell below −121 m at about 25 750 ^{14}C yr BP, but the sea-level change before this time, while indicating falling conditions, is not well defined. The other data from the outer shelf (GC10 and 11) provide comparable results for the Late-glacial period (see Fig. 3) indicating that the sea-level was above −103 m at about 14 570 ^{14}C yr BP.

3. Numerical models for sea-level change for the Sahul Shelf and Bonaparte Depression

The sea-levels from the Bonaparte Depression provide only a first-order estimate of the land-based ice volumes at the time of the LGM. A more rigorous relationship between sea-level and ice volume requires corrections to be made for the glacio-hydro-isostatic contributions to sea-level (Farrell and Clark, 1976; Nakada and Lambeck, 1987) which, for the northwestern Australian region, can amount to about 10% of the observed sea-level, with the magnitude of the correction depending on the distance of the sample site from the present shoreline: The spatial variation of sea-level across the shelf at the time of the LGM can vary by as much as 20 m (cf. fig. 2, Lambeck and Nakada, 1990).

Analyses from tectonically stable areas in different locations around the world, have indicated that an adequate representation of the total isostatic contribution, $\Delta\zeta_I$, to sea-level change can be obtained using relatively simple models of the Earth's rheology. Then, from observations, $\Delta\zeta_{obs}$, of relative sea-level at time, t, the isostatically corrected ice-volume-equivalent, or simply ice-

equivalent, sea-level $\Delta\zeta_{\mathrm{isl}}$ can be written as:

$$\Delta\zeta_{\mathrm{isl}}(t) = \Delta\zeta_{\mathrm{obs}}(\phi, t) - \Delta\zeta_{\mathrm{I}}(\phi, t) \quad (1)$$

where the two terms on the right-hand side are functions of position, ϕ, and time, whereas $\Delta\zeta_{\mathrm{isl}}$ is a function of time only. The ice-volume equivalent sea-level relates to ice volume $\Delta V_{\mathrm{i}}(t)$ by

$$\Delta\zeta_{\mathrm{isl}}(t) = \frac{\rho_{\mathrm{i}}}{\rho_{\mathrm{w}}} \int_{t} \frac{1}{A_{\mathrm{w}}(t)} \frac{\mathrm{d}V_{\mathrm{i}}\,\mathrm{d}t}{\mathrm{d}t}. \quad (2)$$

The theory and model parameterisation used here to compute $\Delta\zeta_{\mathrm{I}}(\phi, t)$ for environments in regions far from the former ice sheets have been discussed in Nakada and Lambeck (1989) and Fleming et al. (1998). For the present computations, the earth models employed assume a three-layered mantle, and Table 4 summarizes a range of earth model parameters that have been found to be consistent with sea-level models and data for other regions. The model E_0 represents parameters found the most appropriate for northern Europe (Lambeck et al., 1998), while model E_3 is more representative of the earth response for eastern Australia (Lambeck and Nakada, 1990).

Because the region of interest lies far from the former ice sheets, the important requirement is that the total change in ice volume is compatible with the change in sea-level at the corresponding time. For the present purpose, the ice models (I_0) for the two hemispheres and the concomitant ice-volume-equivalent sea-level curve discussed in Fleming et al. (1998), are used. The ice models start at the time of the Last Interglacial (OIS 5e)

Table 4
Model parameters used for isostatic calculation[a]

Model	H_1	η_{um}	η_{lm}
E_0	65	4×10^{20}	10^{22}
E_1	50	4×10^{20}	10^{22}
E_2	80	4×10^{20}	10^{22}
E_3	65	2×10^{20}	10^{22}
E_4	65	5×10^{20}	10^{22}
E_5	65	4×10^{20}	5×10^{21}
E_6	65	4×10^{20}	3×10^{22}

[a] H_1 is the thickness (km) of the elastic lithosphere. η_{um} and η_{lm} are the viscosities of the upper (above 670 km) and lower (below 670 km) mantle, respectively.

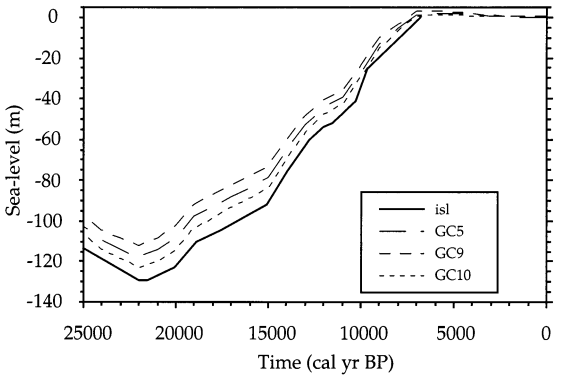

Fig. 6. Relative sea-level curve obtained by glacial-hydro-isostatic modelling for three localities in the Timor Sea for the last 25 ka. GC10 is located at the edge of the continental shelf, whereas GC9 is the site nearest the present-day coastline; GC5 is located in the middle of the Joseph Bonaparte depression.

and ice volume oscillations in the individual ice sheets follow the sea-level function estimated by Chappell and Shackleton (1986).

Fig. 6 illustrates the predicted sea-levels based on models E_0 and I_0 for three localities, GC9, closest to the present continental margin (Fig. 1), GC5 within the Bonaparte depression, and GC10 on the edge of the shelf. All components of the model predictions are the same as those described in Fleming et al. (1998). At all three localities, the local sea-levels are predicted to lie above the isl function, a consequence mainly of the subsidence of the sea floor and the adjacent margin in response to the water loading of the oceanic lithosphere. The differences between predictions for the three localities are significant, and at the site nearest to the present coast, GC9, the sea-level change has always been higher than that for the other two localities. The maximum difference between GC9 and the shelf edge site, GC10, is ca 10 m at the LGM.

Fig. 7 illustrates the changes in sea-level across the shelf relative to present sea-level at three selected epochs, the LGM at 21 000, 13 000 and 7 000 cal yr BP. These curves represent the predicted heights of sea-level with respect to its present level if shorelines could have formed (and been preserved) along the section at the epochs in question. For example, at 21 000 cal yr BP, sea-levels at GC5 would be expected to be shallower

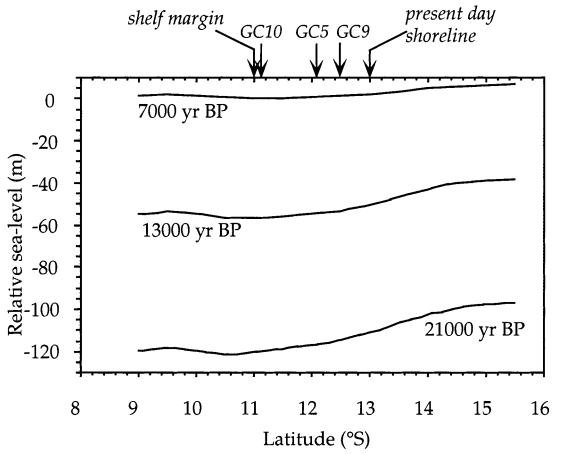

Fig. 7. Inferred height of sea-level across the shelf during three different time intervals.

with respect to the present-day sea-level than the sea-level of the same epoch at GC10, the maximum difference for this choice of model parameters being about 6 m. Uncertainties in the model predictions come from three sources: the choice of earth-model parameters, the ice-sheet parameters, and the assumed equivalent sea-level function. The range of plausible earth-model parameters is summarised in Table 4 and Fig. 8a illustrates the dependence of the predictions for site GC5 on these values. Sea-level predictions for earth model E_6 show the lowest value, whereas the results for most of the others are the same to within ± 3 m. The effects of the earth-model uncertainties are of a similar magnitude for the other two locations in this same time interval (Fig. 8b and c).

Another source of uncertainty in the modelling is the volume of the LGM Antarctic ice sheet. In the model of Nakada and Lambeck (1988), a significant change in Antarctic ice volume was inferred indirectly from a comparison of the northern-hemisphere ice volumes with the observed sea-levels in far-field localities. To examine whether the choice of distribution of ice between the two hemispheres is important in the present context, predictions have also been made for the model E_0 but with an ice model in which there is no change in the southern hemisphere ice sheets, while the northern hemisphere ice volumes have been increased so as to maintain the same equivalent

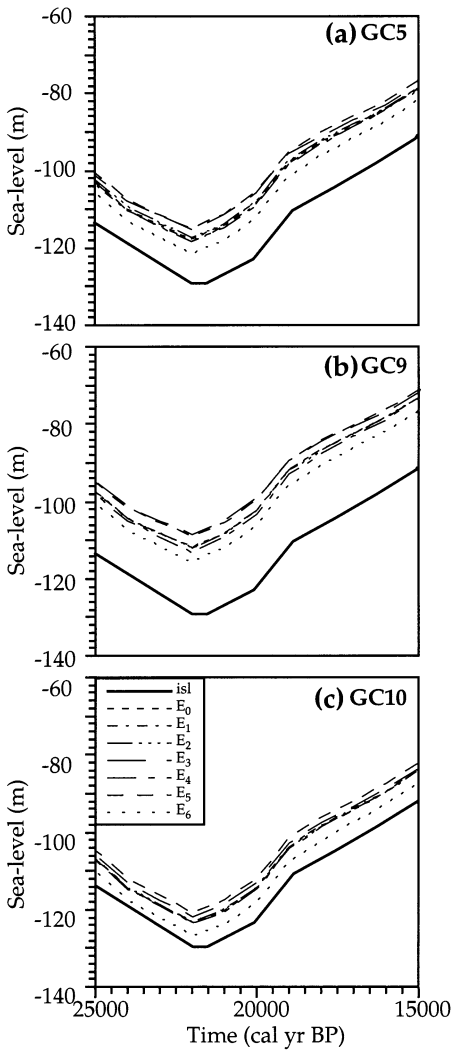

Fig. 8. Dependence of relative sea-level predictions for sites GC5, GC9 and GC10 on the choice of rheological earth-model parameters.

sea-level change as before. Fig. 9 illustrates the results of this comparison. The shallower relative sea-level curve in the figure represents predicted relative sea-level for the standard model of ice distribution in Antarctica. The deeper curve is the predicted relative sea-level curve using the scaled northern hemisphere ice sheet. The maximum difference between the maximum Antarctic ice model and the zero Antarctic-ice model is about 5 m at LGM. Errors in observation of the LGM

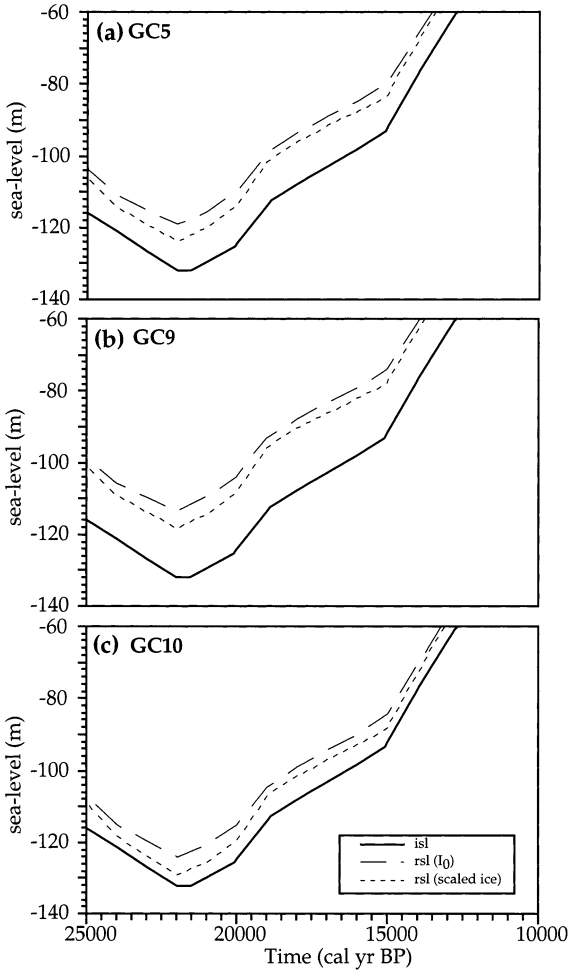

Fig. 9. Evaluation of dependence of sea-level on the choice of geographical distribution of ice. The scaled and total ice model corresponds to zero and maximum Antarctic ice in the model, respectively. The isl is the ice volume equivalent sea-level curve used for calculating two rsl curves. See text for details.

samples are generally of the order of 5 m, so that the sea-level change in the present study may reasonably be taken to be independent of ice volume distribution between the two hemispheres.

4. Inference of the equivalent sea-level change

Fig. 10 depicts the isostatically corrected observations [Eq. (1)] obtained from the Bonaparte Gulf including the results previously published by van Andel and Veevers (1967). For comparison, isostatically corrected Barbados coral data from Fairbanks (1989) and Bard et al. (1990) are also shown where the corrections are based on the same model, E_0 and I_0, discussed above. The bulk of the Barbados data occurs after 19 000 yr BP and corresponds to the age–depth relations of *Acropora* corals that can live in water depths down to 5 m. These results are consistent with the Australian evidence for this period, as are the two older Barbados *Porites* corals that can grow in water depths of up to 20 m. The error bars on the age determinations are all 1 sigma estimates. The ice volume-equivalent sea-level accuracy estimates are given by $(\sigma_{obs}^2+\sigma_{pred}^2)^{1/2}$, where σ_{obs} and σ_{pred} are the standard deviations of the observed sea-level and predicted isostatic corrections, respectively. The observational accuracy cannot usually be defined by normal probability distributions, and estimates of the limiting values are used as a measure of σ_{obs}. The σ_{pred} is half the range of values predicted for the six earth models defined in Table 4.

Also shown in Fig. 10 is the ice-equivalent sea-level function corresponding to the ice models used to predict the isostatic corrections. The comparison with the isostatically reduced observations indicates that the assumed ice model underestimates the total LGM and Late-glacial ice volumes by about 10% and that the predicted isostatic corrections have a further uncertainty of about 10% of their values. With isostatic corrections of the order of 10 m or less, this is small when compared with other error sources, and there is no need to iterate the calculation for $\Delta\zeta_I$.

The early Barbados and Bonaparte data together establish the ice-volume equivalent sea-level at the LGM as being about 135 ± 4 m. The corresponding increase in LGM ice volume over present-day ice volume, using [Eq. (2)], is 52.5×10^6 km^3. The LGM ice volume was maintained from before 22 000 yr BP until 19 000 yr BP, at which time, a rapid rise of about 15 m occurred within less than 1000 years, equivalent to an ice volume discharge of about 5.2×10^6 km^3.

In some estimates of glacial ice volumes, it is the group of Barbados results between 19 000 and 17 000 yr BP that have been assumed to correspond

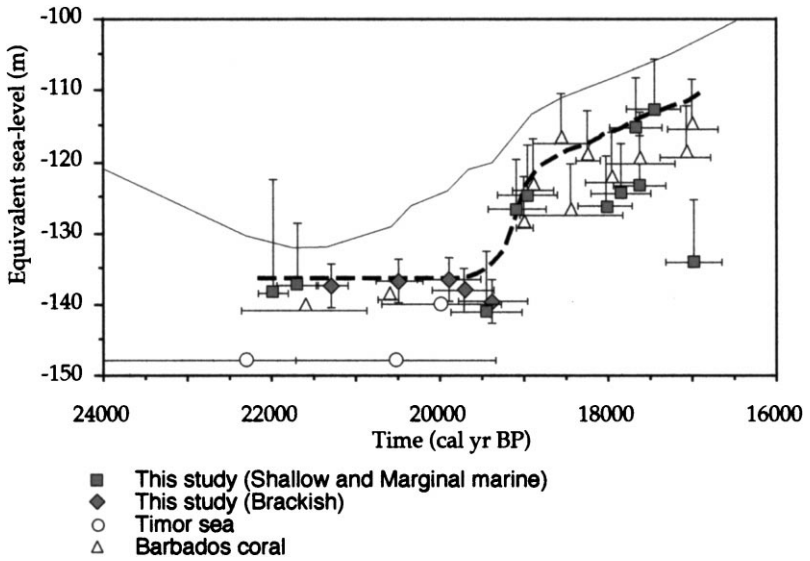

Fig. 10. Ice volume equivalent sea-level value obtained from isostatically corrected observational data. Results obtained from Bonaparte Gulf and Barbados data. The filled symbols are the results from the present study. The continuous line represents the nominal equivalent sea-level curve of glacio-isostatic calculation for the present study. The dotted line is the proposed curve.

to the LGM (e.g. Okuno and Nakada, 1999), whereas the Bonaparte results indicate that the LGM, if defined by the time of maximum ice volumes, corresponds to an earlier period with an abrupt termination at 19 000 yr BP. The two early Barbados observations have sometimes been considered to be unreliable because *Porites* corals can grow in relatively deep water. However, the agreement with the Bonaparte Gulf data indicates that the water depths at the time of growth of these two sampled corals were probably no more than about 5 m and that these two corals are a fair time indicator of LGM sea-level.

The ice volume 52.5×10^6 km^3 (or 135 m ice-equivalent sea-level) can be compared directly with ice volumes determined from glaciological reconstructions. CLIMAP (1981) estimated that ice-equivalent sea-level ranged between 127 and 163 m for their minimum and maximum reconstructions based on the Denton and Hughes (1981) models. The ice-volume estimation from the present study is near the lower range of the CLIMAP values. Peltier (1994) proposed an LGM eustatic value of 105 m and concluded that the CLIMAP ice models contained an excessive amount of ice. However, the model value of eustatic sea-level is not directly comparable with the glaciological estimates of ice volume (Denton and Hughes, 1981), and once the isostatic correction term $\langle \Delta\zeta_I \rangle_{ocean}$ is applied the correspondence is more satisfactory. In fact, the ice-equivalent sea-level change corresponding to 105 m of eustatic change is approximately 135–140 m.

Acknowledgements

We thank John F. Marshall for the opportunity to work on the cores, R. Cresswell and M. di Tada for assisting with AMS measurements, and A. Purcell for assisting with computation. Comments from R.M. Carter and an anonymous reviewer improved the manuscript. Y.Y. was supported by a Ph.D. scholarship from the Research School of Earth Sciences at the Australian National University.

References

Albani, A.D., 1979. Recent shallow water foraminifera from New South Wales. Aust. Mar. Sci. Ass. Handbook 3, 1–57.
Bard, E., Hamelin, B., Fairbanks, R.G., 1990. U–Th ages

obtained by mass spectrometry in corals from Barbados: sea level during the past 130,000 years. Nature 346, 456–458.

Bard, E., Arnold, M., Hamelin, B., Tisnerat-Laborde, N., Cabioch, G., 1998. Radiocarbon calibration by means of mass spectrometric $^{230}Th/^{234}U$ and ^{14}C ages of corals. An updataed data base including samples from Barbados, Mururoa and Tahiti. Radiocarbon 40, 1085–1092.

Burford, M.A., Rothlisberg, P.C., Wang, Y.G., 1995. Spatial and temporal distribution of tropical phytoplankton species and biomass in the Gulf of Carpentaria, Australia. Mar. Ecol. Prog. Ser. 118, 255–266.

Cann, J.H., De Deckker, P., 1981. Fossil Quaternary and living foraminifera from athalassic (non-marine) saline lakes, southern Australia. J. Paleontol. 55, 660–670.

Carter, R.M., Johnson, D.P., 1986. Sea-level controls on the post-glacial development of The Great Barrier Reef, Queensland. Mar. Geol. 71, 137–164.

Chappell, J., Shackleton, N.J., 1986. Oxygen isotopes and sea level. Nature 324, 137–140.

Clapperton, C.M., 1997. Fluctuations of local glaciers 30–8 ka BP: Overview. Quat. Int. 39, 3–6.

CLIMAP Project Members, 1981. In: Seasonal reconstructions of the earth's surface at the Last Glacial Maximum, Geol. Soc. Am. Map Chart Ser. MC-36., 1–18.

Colonna, M., Casanova, J., Dullo, W.C., Camoin, G., 1996. Sea-level changes and $\delta^{18}O$ record for the past 30,000 yr from Mayotte Reef, Indian Ocean. Quat. Res. 46, 335–339.

De Deckker, P., 1988. An account of the techniques using ostracodes in palaeolimnology in Australia. Palaeogeogr. Palaeoclimatol. Palaeoecol. 62, 463–475.

Denton, G.H., Hughes, T.J., 1981. The Last Great Ice Sheets. Wiley, New York. 484 pp.

Fairbanks, R.G., 1989. A 17,000-year glacio-eustatic sea level record: influence of glacial melting rates on the Younger Dryas event and deep-ocean circulation. Nature 342, 637–642.

Farrell, W.E., Clark, J.A., 1976. On postglacial sea level. Geophys. J. 46, 79–116.

Ferland, M.A., Roy, P.S., Murray-Wallace, C.V., 1995. Glacial lowstand deposits on the outer continental shelf of Southeastern Australia. Quat. Res. 44, 294–299.

Fifield, L.K., Allan, G.L., Ophel, T.R., Head, J., 1992. Accelerator mass spectrometry of ^{14}C at the Australian National University. Radiocarbon 34, 452–457.

Fleming, K., Johnston, P., Zwartz, D., Yokoyama, Y., Lambeck, K., Chappell, J., 1998. Refining the eustatic sea-level curve since the Last Glacial Maximum using far- and intermediate-field sites. Earth. Planet. Sci. Lett. 163, 327–342.

Gupta, S.K., Polach, H.A., 1985. Radiocarbon Dating Practices at ANU. Radiocarbon Laboratory, Research School of Pacific and Asian Studies, ANU, Canberra. 173 pp.

Hayward, B.W., Hollis, C.J., 1994. Brackish foraminifera in New Zealand: A taxonomic and ecologic review. Micropaleontology 40, 185–222.

Hughes, T.J., Denton, G.H., Andersen, B.G., Schilling, D.H., Fastook, J.L., Lingle, C.S., 1981. The Last Great Ice Sheets: A global view. In: Denton, G.H., Hughes, T.J. (Eds.), The Last Great Ice Sheet. Wiley, New York, pp. 263–317.

Hurd, D.C., 1973. Interactions of biogenic opal, sediment and seawater in the Central Equatorial Pacific. Geochim. Cosmochim. Acta 37, 2257–2282.

Jongsma, D., 1970. Eustatic sea-level change in the Arafura Sea. Nature 228, 150–151.

Johnson, T.C., 1974. The dissolution of siliceous microfossils in surface sediments of the eastern tropical Pacific. Deep-Sea Res. 21, 851–864.

Lambeck, K., Nakada, M., 1990. Late Pleistocene and Holocene sea-level change along the Australian coast. Palaeogeogr. Palaeoclimatol. Palaeoecol. (Global and Planetary Change Section) 89, 143–176.

Lambeck, K., Smither, C., Johnston, P., 1998. Sea-level change, glacial rebound and mantle viscosity for northern Europe. Geophys. J. Int. 134, 102–144.

Lamprell, K., Whitehead, T., 1992. Bivalves of Australia. Crawford House Press Pty, Bathurst. 182 pp.

McManus, J., Hammond, D.E., Berelson, W.M., Kilgore, T.E., Demaster, D.J., Ragueneau, O.G., Collier, R.W., 1995. Early diagenesis of biogenic opal: Dissolution rates, kinetics, and paleoceanographic implications. Deep-Sea Res. 42, 871–903.

Marshall, J.F., Thom, B.G., 1976. The sea-level in the last interglacial. Nature 263, 120–121.

Murray, J.W., 1991. Ecology and Palaeoecology of Benthic Foraminifera. Wiley, New York. 397 pp.

Nakada, M., Lambeck, K., 1987. Glacial rebound and relative sea-level variations: a new appraisal. Geophys J. Roy. Astron. Soc. 90, 171–224.

Nakada, M., Lambeck, K., 1988. The melting history of the Late Pleistocene Antarctic ice sheet. Nature 333, 36–40.

Nakada, M., Lambeck, K., 1989. Late Pleistocene and Holocene sea-level change in the Australian region and mantle rheology. Geophys. J. Int. 96, 497–517.

Okuno, J., Nakada, M., 1999. Total volume and temporal variation of meltwater from last glacial maximum inferred from sea-level observations at Barbados and Tahiti. Palaeogeogr. Palaeoclimatol. Palaeoecol. 146, 283–293.

Peltier, W.R., 1994. Ice age paleotopography. Science 265, 195–201.

Stirling, C.H., Esat, T.M., McCulloch, M.T., Lambeck, K., 1995. High-precision U-series dating of corals from Western Australia and implications for the timing and duration of the Last Interglacial. Earth Planet. Sci. Lett. 135, 115–130.

Stirling, C.H., Esat, T.M., Lambeck, K., McCulloch, M.T., 1998. Timing and duration of the Last Interglacial: evidence for a restricted interval of widespread coral growth. Earth Planet. Sci. Lett. 160, 745–762.

Stuiver, M., Reimer, P.J., Bard, E., Beck, J.W., Burr, G.S., Hughen, K.A., Kromer, B., McCormac, F.G., Van der Plicht, J., Spurk, M., 1998. INTCAL98 Radiocarbon age calibration 24,000–0 cal BP. Radiocarbon 40, 1041–1083.

Tushingham, A.M., Peltier, R.W., 1991. Ice-3G: A new global model of late Pleistocene deglaciation based upon

geophysical predictions of post-glacial relative sea level change. J. Geophys. Res. 96, 4497–4523.

van Andel, T.H., Veevers, J.J., 1967. Morphology and Sediments of the Timor Sea. Department of National Development: Bureau of Mineral Resources Geology and Geophysics, Canberra.

van Andel, T.H., Ross Health, G., Moore, T.C., McGeary, F.R., 1967. Late Quaternary history, Climate, and Oceanography of the Timore Sea, northwestern Australia. Am. J. Sci. 265, 737–758.

Veeh, H.H., Chappell, J., 1970. Astronomical theory of climatic change: support from New Guinea. Science 167, 862–865.

Vogel, J.S., Southon, J.R., Nelso, D.E., Brown, T.A., 1984. Performance of catalytically condensed carbon for use in accelerator mass spectrometry. Nucl. Instrum. Meth. B 5, 289–293.

Yassini, I., Jones, B.G., 1995. Recent Foraminifera and Ostracoda from Estuarine and Shelf Environments on the Southeastern Coast of Australia. University of Wollongong Press, Wollongong. 484 pp.

Yokoyama, Y., 1999. Sea-level change in Australasia and the radiocarbon time scale calibration during the last 50,000 years. Ph.D. thesis, Australian National University, 229 pp.

Yokoyama, Y., Esat, T.M., Lambeck, K., Fifield, L.K., press. Last ice age millennial scale climate changes recorded in Huon Peninsula corals. Radiocarbon. in press.